SCIE-COM-19028-99-02, Rev. 0

CALCULATION OVERVIEW AND ANALYSIS RESULTS SUMMARY OF THE LOSS-OF-COOLANT INVENTORY SCENARIO IN THE MILLSTONE 1 SPENT FUEL POOL

FEBRUARY 2000

KC Wagner
Jack Dallman

SCIENTECH, INC.

Approved	Signature	Date
R.J. Dallman	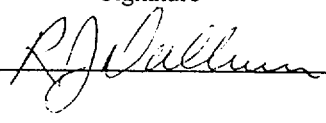	2/25/00

TABLE OF CONTENTS

LIST OF FIGURES

LIST OF TABLES

CALCULATION OVERVIEW AND ANALYSIS RESULTS SUMMARY OF THE LOSS-OF-COOLANT INVENTORY SCENARIO IN THE MILLSTONE 1 SPENT FUEL POOL

1. PURPOSE

The purpose of this analysis was to determine the maximum zircaloy cladding temperature in the Millstone 1 spent fuel pool (SFP) assuming a complete draindown of the pool. In this analysis, the entire coolant inventory of the SFP was assumed to be instantly drained and the fuel was exposed to only air as a coolant. The analysis determined whether the maximum fuel cladding temperature is below an established acceptance criterion for the onset of fuel cladding swelling and rapid exothermic oxidation of the zirconium cladding. The temperature acceptance criterion has been defined as 565°C (1049°F) [1]. If the calculated maximum cladding temperature remains below this temperature, then the fuel cladding will maintain its gross structural integrity. The scenario is based on the decay of the spent fuel from the final shutdown of Millstone Unit 1 through September 1, 1999. If the scenario occurred after September 1, 1999, the peak cladding temperature would be lower due to the natural decrease of the fission product decay heat level with time.

2. ANALYSIS METHODOLOGY/ACCEPTANCE CRITERIA

The analysis of the SFP response to a loss-of-coolant inventory scenario was complicated by several factors. An accurate analysis requires consideration of the interactions between the fuel bundles, the remainder of the SFP, and the Reactor Building (RB) above the SFP. Consequently, the analysis was performed to address each of these three scales. Section 2.1 describes the three-level analyses used to model the range of phenomena present in this analysis. The acceptance criterion was based on a conservative maximum fuel cladding temperature below which fuel clad ballooning and energetic zircaloy oxidation are not expected. The acceptance criterion is described in Section 2.2.

2.1 Analysis Methodology

The primary inputs to the analysis consist of the physical arrangement and contents of the RB and SFP, and the decay heat load. The physical arrangement was modeled using as-built plant information.

The decay heat of the fuel in the SFP was calculated using the ORIGEN2 computer code [5]. ORIGEN2 calculations were made to determine the overall SFP heat load by using batch average values. Fuel from Cycle 1 (discharged on January 9, 1972) through 15 (discharged on November 4, 1995) are present in the SFP [6]. The SFP decay heat load with decay through an assumed date of September 1, 1999 was selected. The limiting bundle selection was based on a

review of the bundle with the highest burn-up and highest batch average decay heat from best-estimate ORIGEN2 calculations.

No single computer code is available to simultaneously model the range of phenomena expected in a SFP loss-of-coolant inventory scenario. Therefore, a three-level analysis methodology that models phenomena on the various length scales was developed to analyze the problem (i.e., (1) bulk building temperatures, (2) SFP flow patterns, and (3) limiting bundle peak cladding temperature).

First, the overall bulk reactor building temperature response was needed. The MELCOR computer code was chosen to perform this analysis [2]. As shown in Figure 2.1, a MELCOR model of the upper level of the reactor building including the SFP was developed. Although the MELCOR model includes the SFP, a lumped approach was used to determine overall bulk heating effects. The MELCOR code calculations evaluate the impact of the ventilation rate and ambient heat loss on the bulk building temperature at the 108'6" elevation. The MELCOR analyses determined the peak bulk RB temperature.

Next, the FLOW-3D® computational fluid dynamics (CFD) code [3] was used to resolve the cooling air flow patterns in the SFP. The FLOW-3D® code permits a detailed three-dimensional analysis of the flow patterns in the SFP. In particular, flow mixing above and below the racks required a fine resolution solution that could be readily simulated by a CFD code. The MELCOR code used a 4-control volume "lumped" approach to model the SFP, while the FLOW-3D® model of the Millstone 1 spent fuel pool utilized 36,000 nodes. The CFD code model addressed concerns about the magnitude of the thermal mixing above the racks, the location of the limiting bundle, and the flow and temperature conditions at the limiting bundle inlet.

Finally, a refined prediction of the highest-powered bundle peak cladding temperature was needed. The FLOW-3D® CFD model included significant detail on the placement of the racks and the obstructions under the racks. However, the resistance and axial power profiles in the bundles were modeled uniformly. In addition, the thermal inertia of the bundles and structures in the SFP were neglected (i.e., all the decay heat was deposited directly into the gas space). This configuration was consistent with quasi-steady conditions once the fuel rods, racks, and other equipment attained their peak temperature. Consequently, the NRC safety research best-estimate thermal-hydraulics code, TRAC-PF1/Mod2 [4] was used to analyze the limiting bundle response. The TRAC-PF1/Mod2 model simulated a single fuel bundle in detail, including the explicit modeling of the powered fuel rods, correct discrete axial placement of the grid spacers and tie plates, and the appropriate axial power peaking factor. The bundle inlet temperature and flow conditions from FLOW-3D® were used as boundary conditions for TRAC-PF1/Mod2.

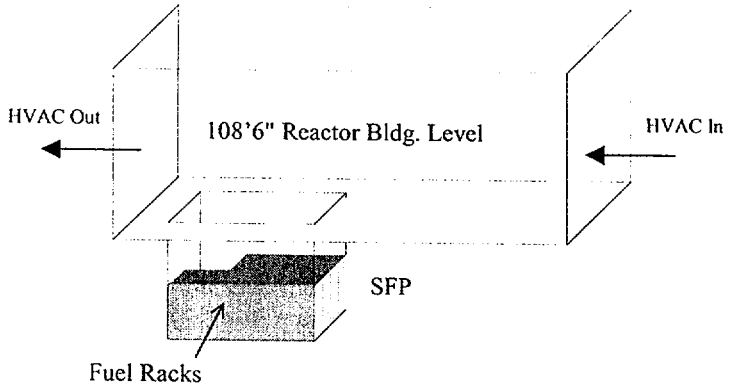

MELCOR Analysis

- Evaluate bulk building temperature response
  - Normal HVAC
  - Ambient heat loss

Bulk room temperature above SFP

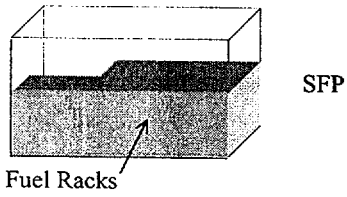

FLOW-3D Analysis

- Detailed 3D analysis of SFP
  - Evaluate 3D flow patterns
  - Evaluate thermal mixing and recirculation flow patterns

Limiting bundle location
- Inlet temperature
- Inlet Resistance

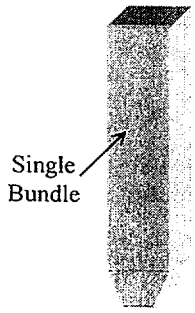

TRAC-PF2 Analysis

- Detailed channel analysis
  - Evaluate peak cladding temperature response

Figure 2.1 Millstone 1 SFP Analysis Methodology.

2.2 Acceptance Criteria

The complete loss-of-coolant inventory scenario was based on the premise that an initiating event could result in the instantaneous loss of water from the SFP. With no water remaining in the pool, only the circulation of air through the spent fuel racks would provide cooling of the fuel. The objective of the analysis is an assessment of resulting peak cladding temperature and comparison of this temperature to an established limit.

If the zircaloy in fuel rod cladding reaches a sufficiently high temperature in a steam or air environment, an exothermic reaction will occur. The NRC gives guidance for the onset of thermal conditions that might lead to a rapid exothermic zirconium reaction in their report on resolution of beyond design basis accidents that could occur in spent fuel pools [7]. In particular, a temperature of 565°C has been used by the NRC staff as the temperature above which the onset of clad swelling could occur. While 565°C is not a sufficient temperature to result in a rapid exothermic zirconium reaction, clad swelling could eventually lead to physical changes that could result in decreased cooling and higher localized cladding temperatures. Consequently, the objective of the present calculations was to evaluate whether the peak fuel cladding temperature in the limiting bundle remained below 565°C.

3. MELCOR BUILDING ANALYSIS

The MELCOR Version 1.8.4 code was chosen to perform calculations of reactor building temperature response to a SFP loss-of-inventory scenario. This section documents the MELCOR reactor building analysis. The following subsections describe the MELCOR code, a description of the key design inputs for the MELCOR model of the SFP and the RB, and the results of the calculation. The peak RB temperature from MELCOR calculation will be used in for the FLOW-3D® SFP and the TRAC-PF1/Mod2 limiting bundle analyses.

3.1 MELCOR Code Description

MELCOR [2] is a fully integrated, engineering-level computer code whose primary purpose is to model the progression of accidents in light water reactor nuclear power plants. The MELCOR code was developed at Sandia National Laboratories for the NRC as a second-generation plant risk assessment tool. A broad spectrum of severe accident phenomena in both boiling and pressurized water reactors are treated in MELCOR in a unified framework. While MELCOR includes models for the nuclear steam supply system (NSSS) response to severe accidents, it has been used extensively by a large, international community to calculate the thermal-hydraulic and fission product response of the reactor building to accident conditions (e.g., Reference 8). It has also received an independent peer review [9]. Consequently, the thermal-hydraulic capabilities of MELCOR make it applicable to the general reactor building heat up analysis that was performed for Millstone 1. Version 1.8.4 (QL) was used for all calculations.

3.2 Key MELCOR Design Inputs

3.2.1 SFP Decay Heat Input

An ORIGEN2 decay heat analysis was performed to determine the total SFP decay heat and the peak batch decay heat [5]. Table 3.1 shows the total SFP decay heat based on the best-estimate ORIGEN2 calculations. The decay heat level for September 1, 1999 was not available from Reference 5. Consequently, a linear interpolation between January 1, 1999 and January 1, 2000 was used. Since the decrease in decay heat follows an exponential decay, a linear interpolation is conservative. As shown in Table 3.1, the total SFP heat load of 1.62 MBtu/hr was used. This value is slightly greater than (but in very good agreement with) the measured Millstone 1 SFP decay heat load of 1.61 MBtu/hr from a test conducted on September 9, 1999 [21].

Table 3.1 SFP Total Pool Decay Heat Level.

Date	Days of Decay	Total SFP Decay Heat [MBtu/hr]
1-Jan-99	1154	1.78
1-Sep-99	1397	1.62[a]
1-Jan-00	1519	1.56
1-Jan-01	1885	1.36

Note (a). Based on a linear interpolation between 1/1999 and 1/2000.

3.2.2 Flow Resistance Calculations

The Millstone 1 SFP contains spent fuel bundles from three GE fuel bundle designs. The key hydraulic differences are the number of fuel rods, the inlet and grid spacer design, and the rod length. The key hydraulic resistance variations are summarized as the 7x7 bundle, 8x8 (144") bundle, and 8x8 (145") bundle [10]. Since the various fuel bundles are distributed throughout the SFP, it was desired to determine the limiting flow resistance that was required for both the lumped MELCOR and CFD SFP analyses. The flow resistance was calculated based on the geometry from the GE fuel bundle drawings [10] for the three fuel designs. The flow resistance for each type of flow bundle was subsequently calculated using the standard single-phase pressure drop equation (e.g., see MELCOR Theory Manual [2]).

$$\Delta P = \frac{1}{2}\rho v^2 \left(f\frac{L}{D} + k \right)$$

The wall friction term, f, was obtained from the Colebrook-White equation that predicts the Moody friction factors across the full range of Reynolds numbers using appropriate laminar and turbulent flow correlations. The flow losses for the grid spacers, tie plates, and nosepiece were taken from Reference 11 and are summarized in Table 3.2.

Figure 3.1 shows the result of the flow resistance calculations for the three bundle types present in the Millstone 1 SFP. The pressure drop results are roughly equivalent for the two 8x8 designs. The fewer number of fuel rods in the 7x7 bundles led to a slightly smaller flow resistance across a wide range of flow velocities. Based on these results, the MELCOR model conservatively used the resistance characteristics consistent with the 145" 8x8 bundles for all bundles represented in the respective models. This also is the appropriate resistance for the highest powered bundle (see Section 5.2).

Table 3.2 MELCOR Bundle Resistance Parameters.

Parameter	Value	Reference
Inlet + Lower Tie-plate K Term[a]	7.56	[11]
7 Grid Spacers K Terms[a]	7 x 1.38	
Upper Tie-plate K Term[a]	1.41	
Number of Rods/Bundle	64	[10]
Number of Bundles	2884	[6]
Flow Area/Bundle [ft^2]	0.111	[10]
Rod Length [ft]	12.1 (Heated) 13.1 (Total)	
Hydraulic Diameter (4 A/P_W) [ft]	0.0452	
Wall Roughness [ft] – Drawn tubing	5e-6	[12]

Note (a). K resistance based on channel flow area.

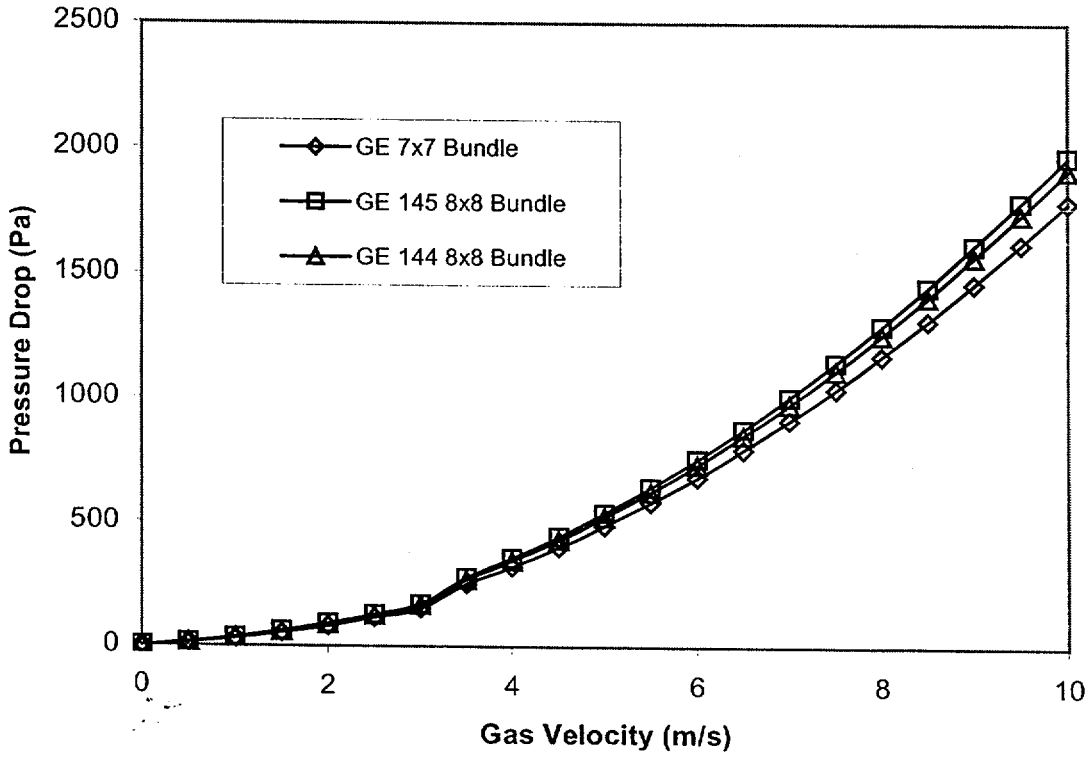

Figure 3.1 Comparison of the Flow Resistance in the Various Bundle Types in the Millstone 1 SFP.

3.2.3 Model Nodalization

A MELCOR model of the Millstone 1 SFP and Reactor Building above the refueling floor was developed for this analysis. The model consists of ten control volumes (CVs), as shown in Figure 3.2. Four CVs represent the SFP. CV 203 represents the space containing the spent fuel and racks. This CV spans in elevation from the SFP floor at 69'9" to the top of the tallest rack at 84'2". CV 202 represents the area from 69'9" to 84'2" (elevation) in the Northeast corner of the SFP that does not contain fuel or racks. CVs 201 and 204 represent the remainder of the SFP from elevation 84'2" to 108'6", with CV 201 containing the volume directly over CV 202 (open area) and CV 204 containing the volume directly over the spent fuel racks contained in CV 203. The SFP nodalization was defined based on an anticipated flow of cool air downward through the open areas of CVs 201 and 202, cross flow underneath the fuel racks and upward cooling flow through the fuel bundles in CV203, and a rising thermal plume through CV 204 and into the RB above the refueling floor.

Five CVs are used to represent the RB above the refueling floor (i.e., above the 108'6" level). The portion of the RB below elevation 108'6" was conservatively neglected in the MELCOR model. CVs 101 through 104 represent the four quadrants of the RB between the refueling floor (i.e., the 108'6") to 129'6"(i.e., halfway between the refueling floor elevation and the top of the RB), while CV105 models the region above 108'6". The partitioning of the RB into CVs at two elevations was intended to allow potential modeling of thermal stratification that might affect the temperature of air entering the fuel bundles. CV 102 represents the Northwest portion of the RB directly over the SFP. CV 101 represents the portion directly East of the SFP, where the equipment hatch enters the 108'6" elevation of the RB. This flow path provides a connection to the environment (CV 002) through the railway door at the 14'6" elevation. CV 103 represents the portion of the RB directly south of the SFP, and the CV104 represents the remaining southeast portion of the RB. CV 105 contains the tornado damper flow path (for seven dampers) to the environment, which could be opened for a failed HVAC scenario[1]. Finally, CV 002 was used to model the environment outside of the reactor building.

As shown in Figure 3.3, HVAC supply flow is modeled with Flow Paths 201 and 202, and exhaust is modeled with Flow Paths 203 and 204. The HVAC supply flow paths were defined as constant velocity flow paths, with the velocity set to supply the desired HVAC flow. The exhaust flow paths were modeled to maintain the appropriate mass flow balance by specifying a quarter-inch pressure drop across the flow path.

The concrete walls and floors were modeled as heat sinks for the RB 108'6" elevation, with a convection boundary condition applied on each surface of these structures. In addition, the insulated metal roof with 4-ply built up roofing (to the 108'6" RB elevation) was modeled. The

[1] The flow paths representing the equipment hatch and railroad door were not used in the present analysis. The flow paths were included to permit alternate scenario progressions where a natural circulation flow pattern to the environment was included.

stainless steel lined, concrete structure of the SFP was also modeled as a heat sink with a conservative adiabatic boundary condition on the outer surface.

The spent fuel is approximated as a cylindrical fuel rod with a surface area scaling factor equal to the total number of rods stored in the pool (169,452 rods from 2884 bundles [6]). The UO_2 pellet, the helium gap, and the zircaloy cladding are all modeled as part of this heat structure. The decay heat is specified as a constant internal power source (to the UO_2 pellet) with a total power equal to the total SFP decay heat for the assumed date of the postulated scenario.

3.2.4 Modeling Assumptions and Conservatisms

Several assumptions were made during the development of the MELCOR model for this analysis. These assumptions are listed below.

1. The reactor building volumes and structures below elevation 108'6" other than the SFP, and those outside the RB above the refueling floor were neglected in this analysis. A significant amount of thermal inertia was ignored that would provide a heat sink as the overall RB temperature rises. Consequently, this assumption is considered conservative.

2. The thermal capacities of the fuel racks, water rods in the fuel bundles, miscellaneous equipment in the RB, and structures in the RB were conservatively neglected. The only heat transfer mechanisms for structures are convection to the walls, ceilings and floors of the SFP and the spent fuel storage room.

3. The flow through fuel racks was conservatively modeled for maximum resistance using 8x8-fuel bundle geometry (see Section 3.2.2).

4. The fuel heat structure geometry was modeled as if all fuel bundles were the 8x8 design with a single water rod. When applying the total decay heat load to these heat structures, this conservatively resulted in the maximum amount of heat generation per unit mass.

5. The flow length under the fuel racks was modeled as the length from the periphery of the pool to the pool center.

6. Although HVAC system specifications require the RB to be kept at a temperature under 33°C (92°F)[2], the RB was initialized to a temperature equal to the assumed limiting-case summer environmental conditions (41°C (105 °F) and 50% RH) [13]. HVAC inlet flow is assumed to have the same thermodynamic characteristics as the outside environment. No credit is taken for active cooling of the HVAC supply.

[2] Temperatures are reported in Celsius throughout the report to facilitate comparison with the peak fuel cladding temperature acceptance criteria, which is commonly reported as 565°C. The equivalent Fahrenheit temperature is also included for reference.

7. The heat transfer calculations to the RB outside walls conservatively assumed a stagnant, no wind condition.

8. The total HVAC supply flow to the reactor building is 108,800 cfm [14]. However, at this nominal flowrate, only 22,700 cfm is supplied to the 108'6" elevation. Since the MELCOR model only represented the region above 108'6", the HVAC flows in the MELCOR model were based on 22,700 cfm as 100% HVAC flow.

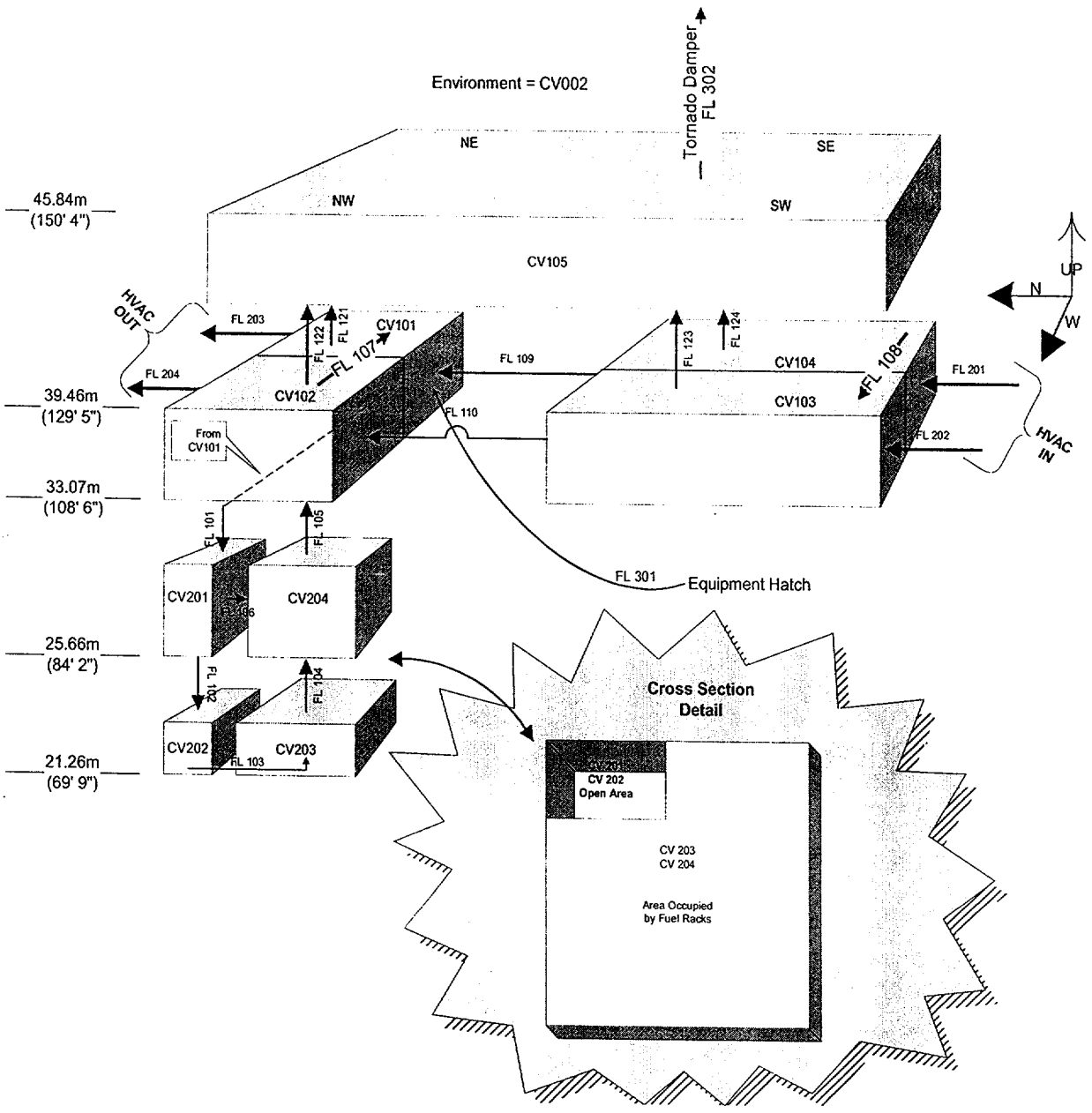

Figure 3.2 **MELCOR Nodalization for the 108'6" Floor of the Millstone 1 Reactor Building.**

3.3 MELCOR Calculations

The MELCOR calculation began by assuming instantaneous draining of the SFP. The bulk gas temperature of MELCOR Control Volume 101 was monitored, as it is the source temperature for the FLOW-3D® CFD calculation. When the CV101 bulk gas temperature reached a peak value, the calculation was stopped. As shown in Figure 3.3, the peak temperature for CV101 was 69°C (156°F). Due to robust mixing of the thermal plume leaving the SFP with air in the 108'6" level, the peak temperature and temperature history of CV101 closely followed (i.e., ±1°C or ±2°F) the other CVs above the SFP.

The time history for the RB temperature in CV101 is presented in Figure 3.3. Due to the relatively low level of decay heat in the SFP, it takes approximately 8 days to achieve 90% of the temperature rise. Subsequently, the rate of temperature increase slows and the RB temperature gradually creeps toward a balance of the SFP heat load versus the HVAC heat removal and the ambient heat loss. As shown in the figure, this balance takes about 50 days to achieve. By 50 days, the temperature rise had essentially stopped and the air temperature stabilized near 69°C (156°F)[3]. It is important to note that diurnal variations in the outside temperature were not included in the MELCOR calculation. Consequently, it was very conservatively assumed that the outside air remained at the maximum daytime temperature. This is extremely conservative, given that it represents conditions more severe than actually possible at the Millstone site.

An evaluation of the heat balance at the final steady state conditions showed that 70% of the SFP heat load was removed by the HVAC and 30% was removed by natural convection heat losses through RB walls and roof. The ambient heat loss was driven by the 32°C (57°F) temperature difference from inside the RB to the environment.

[3] The temperature rise in the last week of the calculation was <0.1°C/week (0.2°F/week).

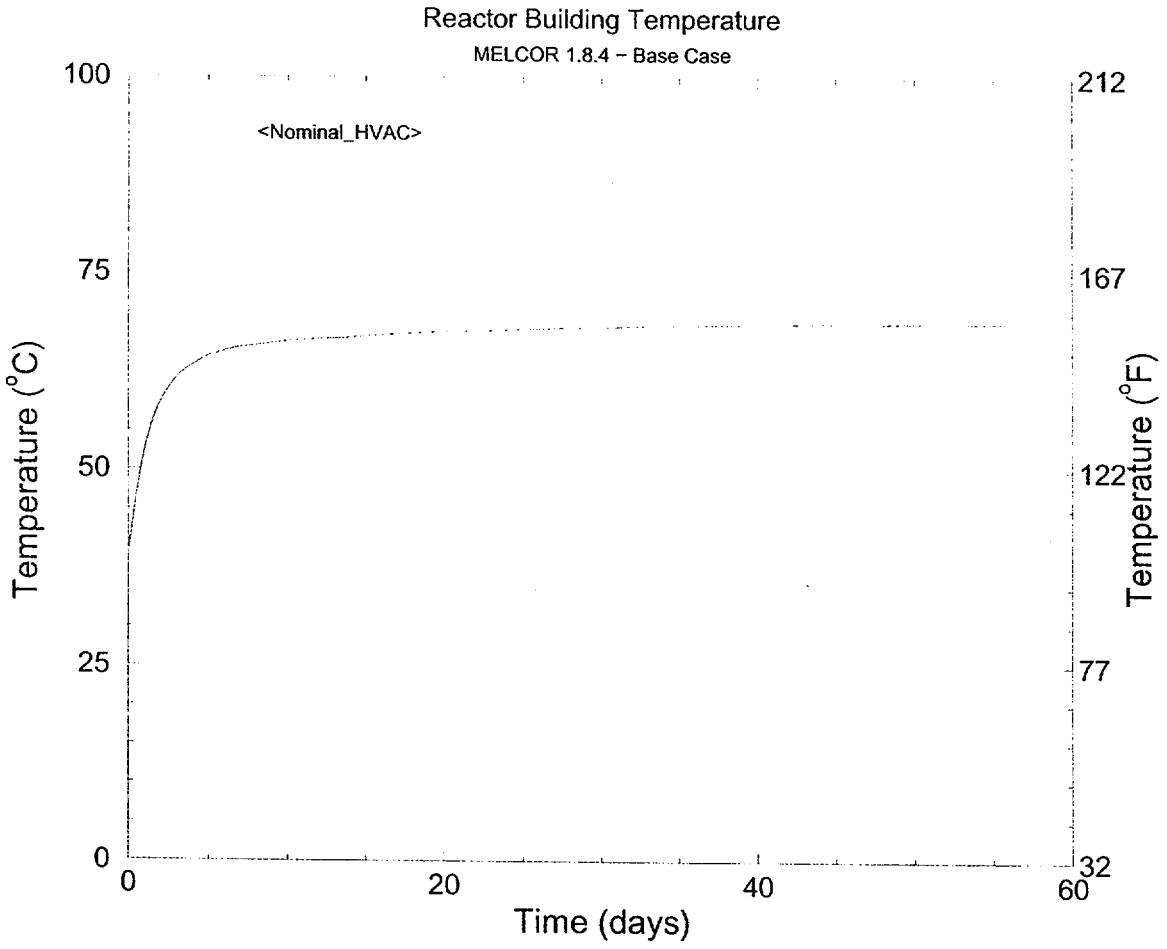

Figure 3.3 MELCOR Building Temperature Response.

4. FLOW-3D® THREE-DIMENSIONAL CFD ANALYSIS OF THE SFP

The FLOW-3D® CFD code was used to resolve the three-dimensional flow distribution in the SFP. The peak building temperature from the MELCOR calculation (i.e., the temperature of CV101 in Figure 3.2) was used to specify the temperature condition at the top of the pool in the FLOW-3D® calculation. Upon obtaining "steady-state" temperature/fluid field conditions in the FLOW-3D® simulation, the flow and temperature at the inlet to the hottest bundle was used to drive the TRAC-PF1/Mod2 calculation. The following subsections provide a description on the FLOW-3D® code, the model of the SFP, and the results obtained with FLOW-3D®.

4.1 FLOW-3D® Code Description

FLOW-3D® [3] is a general-purpose, commercially available CFD code designed to compute the time-dependent behavior of both compressible and non-compressible fluids in one, two, and three-dimensional space through the solution of the coupled mass, momentum, and energy field equations. Since the code solves the fundamental laws of mass, momentum, and energy conservation, it is referred to as a "general purpose" solver. NRC contractors and utilities have applied the FLOW-3D® code to a wide array of reactor safety issues. Some key features of FLOW-3D® that are important for this SFP analysis include: viscous stress and κ-ε turbulent models, variable density buoyant flow models, and models for flow through porous media. Version 7.1.2 was used for all calculations.

4.2 Key FLOW-3D® Design Inputs

4.2.1 Model Description

The Millstone 1 Spent Fuel Pool (SFP) measures 40'4" from the east to west walls, and 36'6" from the north to south walls. The obstacle layout modeled with FLOW-3D® is shown in Figure 4.1 [15]. Specifically, three major rack modules were modeled: two Boraflex rack configurations, and one "Super-Module". The rack module designated by "Boraflex Racks – II" was split into two regions: one powered and one unpowered. The unpowered region contains new fuel and control rod blades. As shown in the figure, the gaps between the modules were modeled explicitly [15]. The number of mesh nodes in the x-, y-, and z-direction were 40, 30, and 30, respectively.

The resistances and flow areas used for each module were based on the assumption that each bundle was a GE 8x8 (heated length of 145"). The flow areas within the racks in the x-, and y-directions were set to zero, and the z-direction flow area up the channels was determined based on both bundle and rack flow restrictions [10 and 16]. The same flow areas and resistances were used for both the Super-Module and the Boraflex racks. The combined losses from wall friction, the seven grid spacers, the nose piece, and upper and lower tie plates [11] were explicitly included.

The areas designated as "Hot Bundle" regions were modeled as separate obstacles in FLOW-3D®. Two of the regions contained a single row of 6 bundles (the width of the interior rack on either side of the Super-Module), and the other region contained a 4-by-4 block of bundles located at the farthest position from the large open cask area, where the largest source of cold air down-flow exists. The flow areas and resistances utilized for these regions were based on the same values as those used for the average regions.

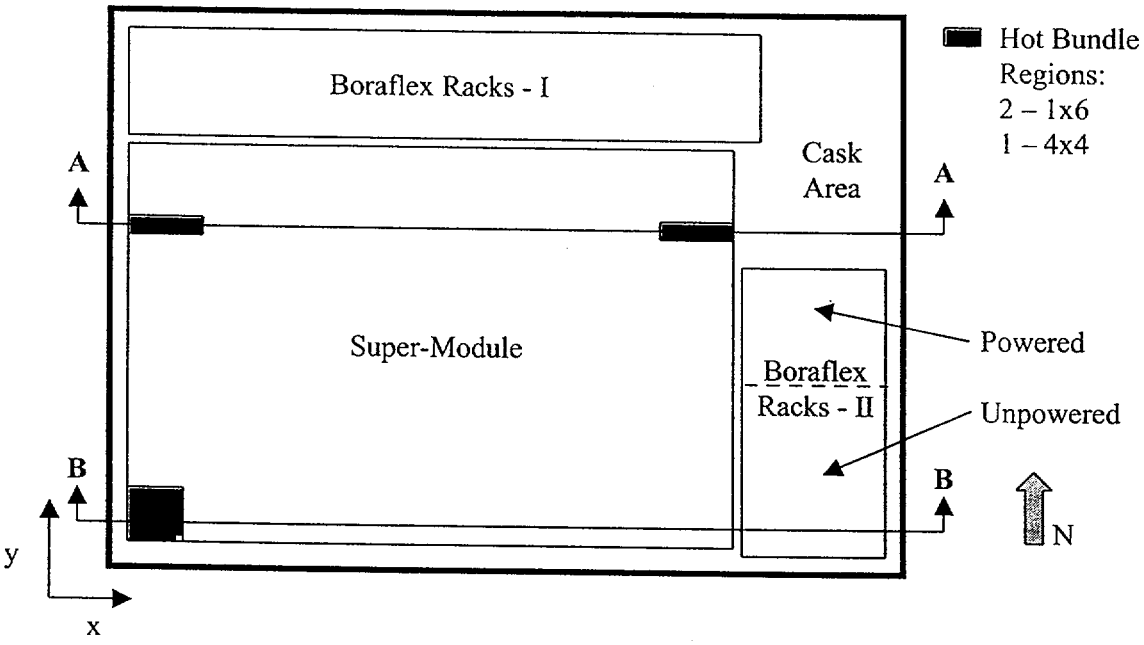

Figure 4.1 Plan View of SFP Obstacle Model.

The total SFP heat load modeled in FLOW-3D® was based on the September 1, 1999 value of 1.62 MBtu/hr shown in Table 3.1, which came from best-estimate ORIGEN2 calculations [5]. The total heat load was divided over 2129 bundles in the Super-Module, 534 bundles in "Boraflex Racks – I", and 221 bundles in "Boraflex Racks – II". The decay heat values for the hot bundle regions were taken from the decay heat of the hottest batch offloaded at the end of Cycle 15 (i.e., the LYH batch). The hot bundle decay heat, also calculated for September 1, 1999, was 1276 Btu/hr/bundle (see Section 5.2.2).

Section A-A and Section B-B from Figure 4.1 are shown in Figures 4.2 and 4.3, respectively. A constant temperature/pressure boundary condition was used at the top of the SFP, where the

temperature was taken to be 77°C (170°F)[4]. The gap under the Boraflex racks is 6" [17] and was assumed to be completely unobstructed. The gap under the Super-Module, however, is somewhat more complicated due in large part to the complex support structure underneath these racks. From the drawings [16], the obstruction area caused by the feet and support beams under the racks resulted in an average porosity of 0.482 in the x- and y-directions, and an average porosity of 0.725 in the z-direction. These average porosities were based on the gap height of 9.8" (to the bottom of the racks). In addition, flow wall friction was applied to the flow under the racks based on a floor roughness of commercial steel [12].

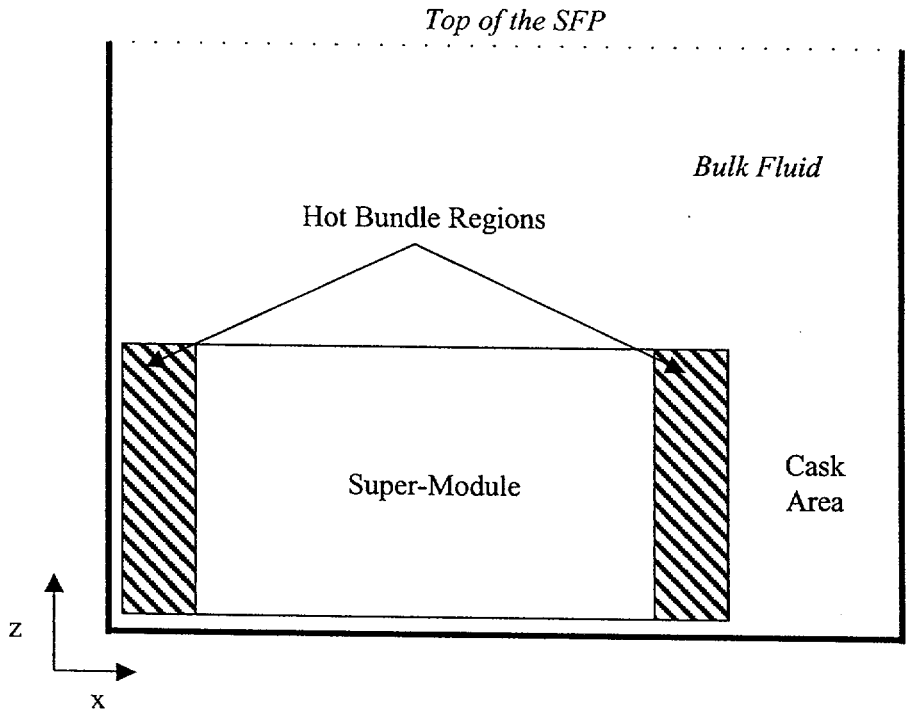

Figure 4.2 Section A-A of Figure 4.1.

[4] A representative bulk building temperature of 170°F (350 K) was used as the boundary condition for the FLOW-3D® calculation. This temperature is slightly above the peak temperature from the MELCOR calculation described in Section 3 and representative of the bulk air properties expected above the SFP. It is important to note that the absolute temperature values from the FLOW-3D® calculations were not used in the peak cladding temperature evaluations. Rather, only the temperature rise from the bulk temperature to the limiting channel inlet was taken from the FLOW-3D® calculation. The TRAC-PF1/Mod2 calculations presented in Section 5 combined the temperature rise from the FLOW-3D® calculation with the peak bulk temperatures calculated by MELCOR to specify the limiting channel inlet condition.

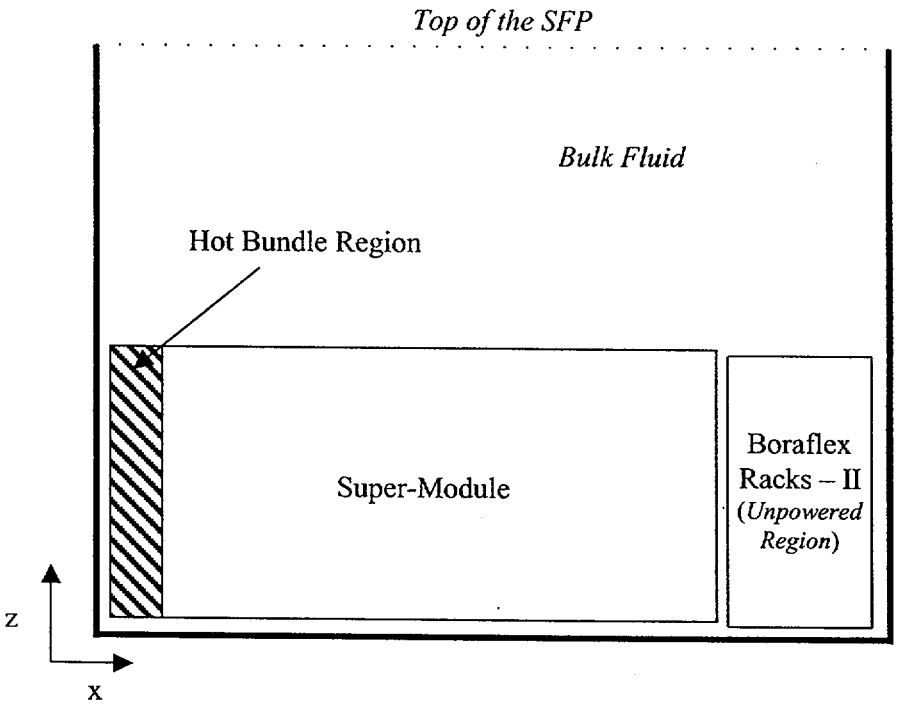

Figure 4.3 Section B-B of Figure 4.1

The selection of the location of the hot bundle regions was made based on a scoping calculation performed with average-powered bundles everywhere in the SFP. From this calculation, it was determined that the hottest region was located at the leading edge of the Super-Module next to the cask area (1x6 region on the right side of the Super-Module in Figure 4.1). A brief discussion of why this region is the hottest is presented in the following section. The additional two hot regions were modeled to ensure that the limiting region was being modeled with the hottest bundle. These locations were also identified as potential trouble spots due to low-flow conditions in the scoping calculation.

4.2.2 Modeling Assumptions and Conservatisms

Several assumptions were made during the development of the FLOW-3D® model for this analysis. These assumptions are listed below.

1. Since the FLOW-3D® analysis was performed, the new fuel has been removed from the Millstone 1 SFP. The removal of the new fuel will increase the airflow into the racks from the Southeast corner of the SFP (i.e., the unpowered "Boraflex Racks - II") and reduce the

airflow from the Northeast opening. As will be shown in the FLOW-3D® results, the peak cladding temperature was strongly influenced by a Bernoulli effect on the leading bundle on the northeast corner of the SFP. The addition of a large downward airflow path in the Southeast region of the SFP will reduce the airflow velocity on the Northeast side and the SFP peak cladding temperature.

2. No structural or wall heat transfer was modeled in the FLOW-3D® model. Consequently, all the decay energy went into the air. In reality, some of the decay heat energy would be absorbed into the concrete walls. The current approach conservatively maximizes the heat load to the air providing the cooling in the SFP.

3. There were several locations throughout the pool that were empty or contained control blades. These locations were modeled as having the 8x8 bundle resistance. In addition, all the 7x7 bundle locations were assumed to have the resistance associated with the 8x8 bundles.

4. Initially, scoping calculations were performed to identify the limiting bundle location. As shown in Figure 4.2, high-powered bundles were placed in these locations. In reality, the highest-powered bundles are not at the limiting location [18].

5. The Renormalized Group (RNG) Theory κ–ε model for flow turbulence was used in the simulation. The inclusion of flow turbulence increases the overall flow resistance and enhances thermal mixing. The RNG model is the recommended turbulence model in FLOW-3D® and does not require user input for equation constants. Instead, the equation constants are derived explicitly. The RNG model is known to accurately describe low intensity flows and flows having strong shear regions (e.g., near the outlet of the bundles) [3].

6. The bundle flow losses included grid spacers and wall friction. However, it was assumed that the resistance was uniformly distributed across the axial length of the bundle. TRAC-PF1/Mod2 single bundle model calculations (described in Section 5) were performed to better refine the actual bundle resistance distribution.

7. The decay heat was uniformly spread across the porous media regions representing the fuel bundles. Since there were gaps between the fuel bundles, the resulting power density was lower than the TRAC-PF1/Mod2 single bundle model calculations (described in Section 5). However, the total SFP decay heat power was conserved. TRAC-PF1/Mod2 calculations were subsequently performed to better refine the actual limiting bundle power density, radial power distribution, and fuel rod response.

8. A porous media model was used to represent the resistance through and under the racks. Flow resistances (i.e., wall friction and flow loss terms) and average porosities were calculated to represent these complex regions. Explicit mesh boundaries were placed at the

edges of the modules to accurately represent the open regions in the SFP. TRAC-PF1/Mod2 single bundle model calculations (described in Section 5) were performed to better refine the actual geometry of the limiting bundle. The porous media approximations were assumed to adequately characterize the flow resistance of the SFP structures.

4.3 FLOW-3D® Calculations

Figure 4.4 depicts the bulk temperature profile and velocity vectors in a x-z slice located at y=0.435m, which corresponds to Section B-B of Figure 4.1. The peak temperature in this slice is 229°C (444°F), which is located near the exit of the corner bundle.

Figure 4.5 depicts the bulk temperature profile and velocity vectors in a x-z slice located at y=5.614m, which corresponds to Section A-A of Figure 4.1. The peak temperature in this slice is 240°F (464°F), which is located near the exit of the bundle near the leading edge of the Super-Module. This temperature, which is the peak for the entire SFP, is highest in this location largely because the up-flow through this bundle is the smallest. As can be seen in the figure, the air velocity under the racks at the leading edge is significantly larger than elsewhere in the pool. This large velocity induces a so-called "Bernoulli effect", which reduces the flow up the bundles near the leading edge.

This point is demonstrated by Figure 4.6, which shows the x-direction velocity under the racks. At the leading edge, the velocity is largest with a value of approximately 9.8 ft/s (3.0 m/s)[5]. As can be seen in the figure, the velocity from the leading edge diminishes along the bottom until it encounters flow in the opposite direction, which originates from the down-flow through the gap near the left wall. The reduction of flow in the (-)x-direction is caused by radial flow spreading and upflow into the bundles. As can be see in Figure 4.6, the bundles to the west (i.e., left) of x=7.5 ft (2.3 m) are supplied by flows from the gap on the west side of the racks while the bundles to the east (i.e., right) of x=7.5 ft (2.3 m) are supplied by flows from the east side of the racks.

[5] In contrast, the flow under the racks in the Southwest corner of the SFP (i.e., the location of the high-powered bundles in Section A-A) is only 3.2 ft/s (1 m/s) and the bundle inlet flow was much higher.

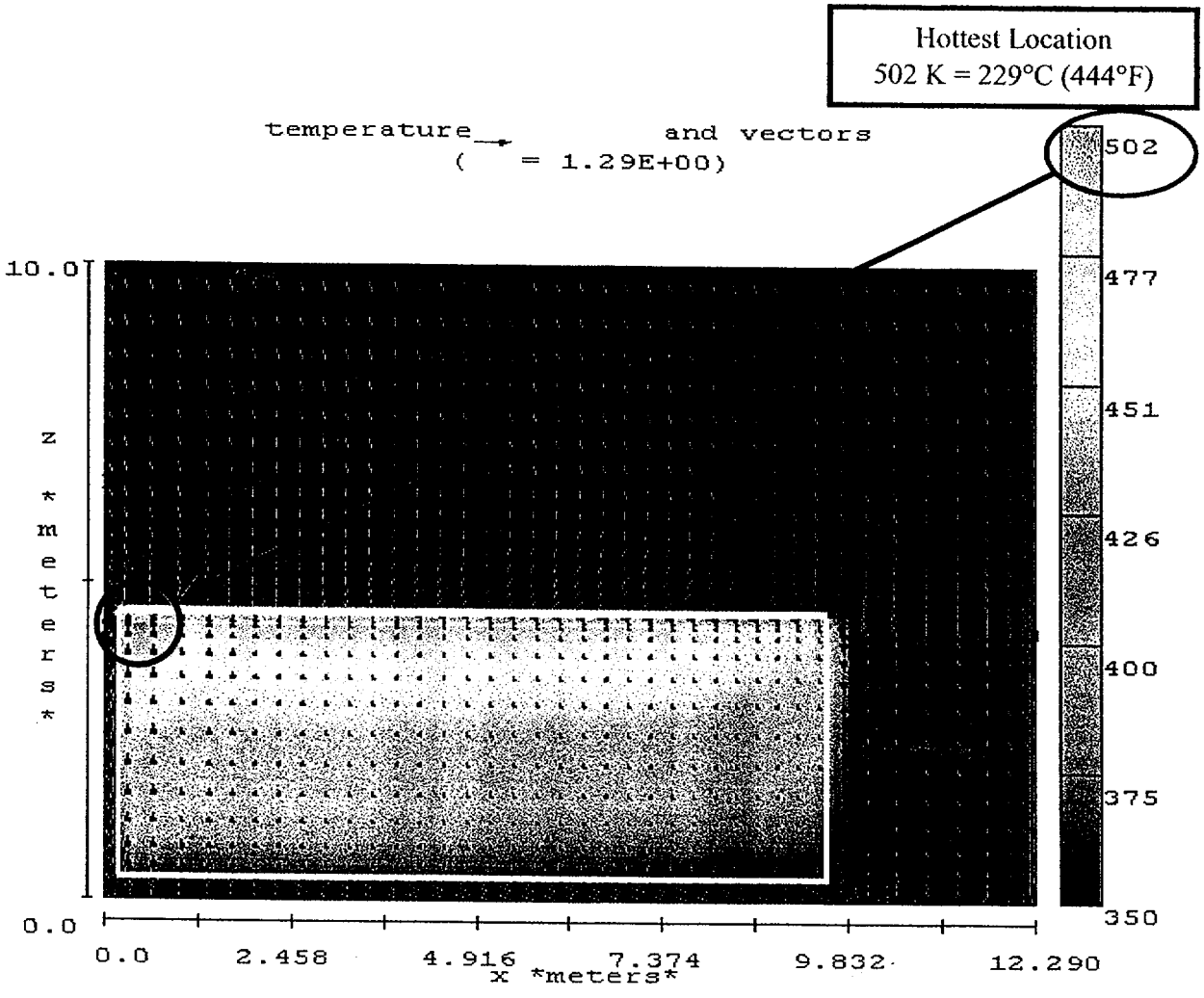

Figure 4.4 X-Z Temperature Profile with Velocity Vectors at Y=0.435 m[6].

[6] The FLOW-3D™ two-dimensional figure shows temperature (in color according to the scale on the right) and flow vectors. The temperature is output in Kelvin. The appropriate temperature conversions to Celsius and Fahrenheit are indicated on the figure. The outline of the Super-Module is shown as a white box. The peak temperature location is indicated for reproductions of this report that are in black and white.

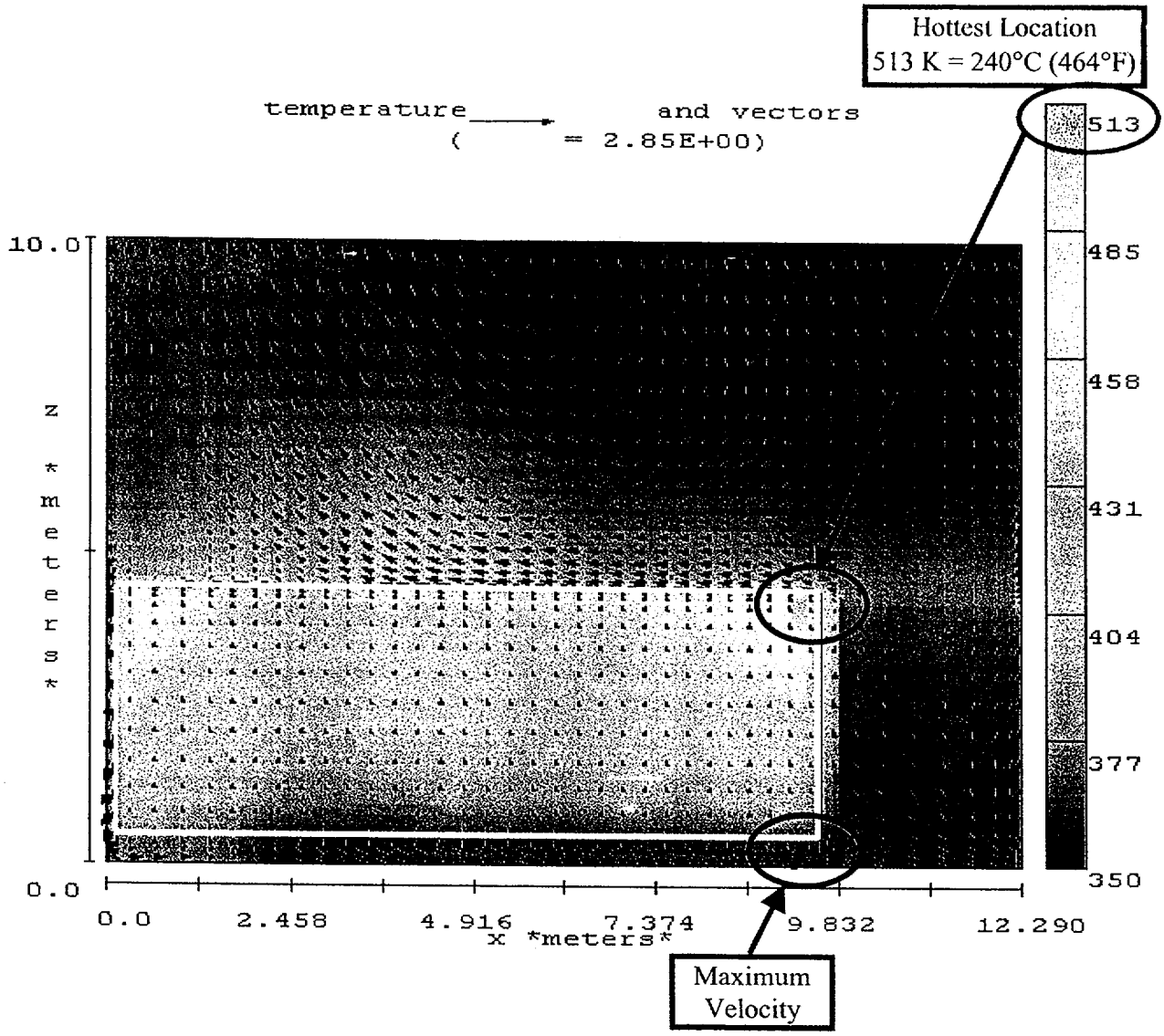

Figure 4.5 X-Z Temperature Profile with Velocity Vectors at Y=5.614 m.[7]

[7] The FLOW-3D™ two-dimensional figure shows temperature (in color according to the scale on the right) and flow vectors. The temperature is output in Kelvin. The appropriate temperature conversions to Celsius and Fahrenheit are indicated on the figure. The outline of the Super-Module is shown as a white box. The peak temperature location is indicated for reproductions of this report that are in black and white.

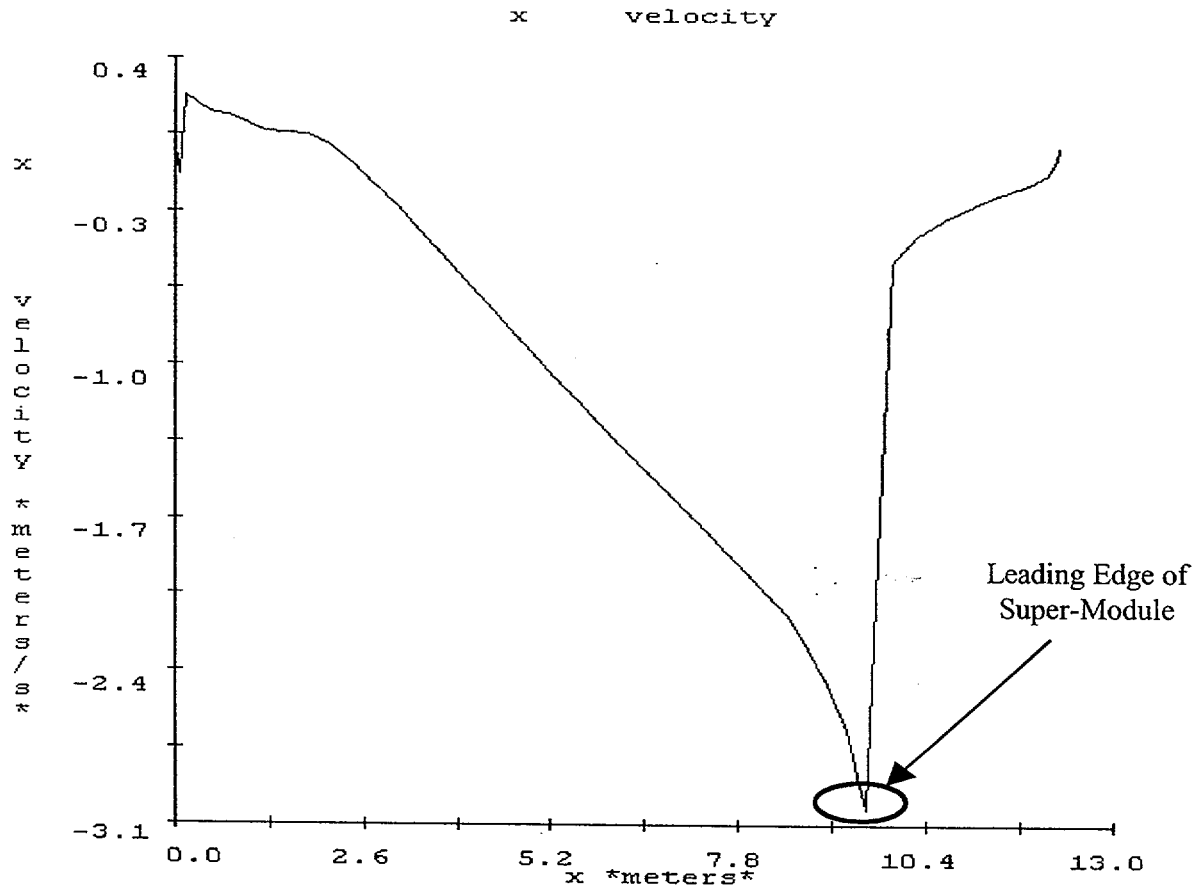

Figure 4.6 X-Velocity Under the Super-Module at Y=5.614 m[8].

A quasi-steady temperature and flow profile was quickly established in the calculation, and the bundle on the leading edge to the Northeast opening had the hottest exit temperature. The flow and inlet conditions at this "limiting" bundle location had stable conditions that were used to specify the inlet conditions for the TRAC-PF1/Mod2 calculation. Table 4.1 summarizes the key results from the FLOW-3D® calculation. In particular, the temperature at the inlet to the limiting bundle shows some mixing of the bulk fluid above the SFP with hot gases exiting the fuel bundles (i.e., a 11°C (20°F) temperature rise). Due to the "Bernoulli effect" from the high-speed flow under the limiting bundle, the inlet flow was restricted to 0.49 ft/s (0.15 m/s). The resultant temperature rise in the limiting bundle was 153°C (275°F).

[8] The FLOW-3D® velocity versus X-position under the super modules shows gas velocity in [m/s]. The peak velocity location is indicated on the figure and occurs at the leading edge of the Super-Module.

Table 4.1 Limiting Bundle Steady Sate Results.

Parameter	Value
SFP Bulk Temperature	77°C (170°F)
Limiting bundle Inlet Temperature	88°C (190°F)
Temperature rise (ΔT) to limiting bundle inlet	11°C (20°F)
Bundle Temperature Rise	153°C (275°F)
Limiting bundle outlet temperature	240°C (464°F)
Bundle inlet velocity	0.49 ft/s (0.15 m/s)

5. TRAC-PF1/MOD2 ANALYSIS LIMITING BUNDLE ANALYSIS

The Transient Reactor Analysis Code-PF1/Mod2 (TRAC-PF1/Mod2) was chosen to perform calculations of fuel rod heatups in the SFP. This section documents the TRAC-PF1/Mod2 limiting bundle analysis. The following subsections describe the TRAC-PF1/Mod2 code, the key design inputs for the TRAC-PF1/Mod2 limiting bundle model, and the results of the calculations. The peak cladding temperature from the TRAC-PF1/Mod2 calculations will be compared to the acceptance criteria for the minimum cladding temperature that might lead to a sustained rapid oxidation reaction.

5.1 TRAC-PF1/Mod2 Code Description

TRAC-PF1/Mod2 is an advanced best-estimate systems code for analyzing transients in thermal-hydraulic systems [4]. TRAC-PF1/Mod2 has been designated by the NRC as its large break loss-of-coolant accident (LOCA) computer code. It is also appropriate for small break LOCAs and transients. The phenomena and physics governing a loss of water accident in a SFP are very similar to those expected in a reactor LOCA. The key applicable models in TRAC-PF1/Mod2 include single-phase flow and heat transfer, two-dimensional structural heat transfer, non-condensable gas field, and cladding oxidation. TRAC-PF1/Mod2 has been used extensively in the predictions and code/data comparisons of experiments and for NSSS simulations. Version 5.28 of the code was used for all calculations.

The complete loss-of-coolant inventory at very low airflows is not a typical simulation for the TRAC-PF1/Mod2 code. In fact, it's sophisticated two-phase flow and heat transfer models are not required for this configuration. However, a review of the basic single-phase flow and heat transfer models show that they are directly applicable for this configuration. The wall friction model used in TRAC-PF1/Mod2 is Churchill's wall drag correlation [4]. Churchill's correlation is a fit to the Moody curves, which include the laminar, transition, and turbulent smooth and rough flow regimes. As will be shown in Section 5.3, the limiting bundle is in laminar flow. Since the Churchill equation includes laminar flow resistance and the abrupt entrance, tie-plate, and grid spacer losses are independent of Reynolds Number, the resistance model in TRAC-PF1/Mod2 is appropriate. In addition, as will be shown in Section 5.3, the peak cladding temperature is not very sensitive to bundle losses due to the high-pressure drop from the Bernoulli effect beneath the racks. Consequently, the exact magnitude of the laminar bundle resistance does not significantly affect the peak cladding temperature.

The single-phase vapor wall heat transfer coefficient (HTC) is the larger of either the turbulent natural-convection HTC or a turbulent forced-convection HTC obtained from the empirical correlation of Sieder and Tate [19]. It might appear that the TRAC-PF1/Mod2 turbulent single-phase HTC would maximize the cladding to air heat transfer. However, as will be shown in Section 5.3, the peak cladding temperature is not very sensitive to the magnitude of the HTC. In fact, the HTC calculated by TRAC-PF1/Mod2 is conservative (i.e., low) relative to a more appropriate laminar HTC.

5.2 Key TRAC-PF1/Mod2 Design Inputs

The key design inputs for the TRAC-PF1/Mod2 model are discussed in this section. First, a nodalization description is given in Section 5.2.1. The key boundary conditions, decay heat and inlet flow and temperature, are discussed separately in Sections 5.2.2 and 5.2.3, respectively. Finally, a list of assumptions used in the TRAC-PF1/Mod2 model analysis is summarized in Section 5.2.4.

5.2.1 Nodalization Description

The TRAC-PF1/Mod2 model relies entirely on the development of natural circulation from buoyancy forces to circulate air through the storage cells. The TRAC-PF1/Mod2 model represents a single fuel bundle with inlet conditions and decay power consistent with the highest-powered bundle in the limiting location[9]. The single bundle model was conservatively modeled with an adiabatic boundary.

The nodalization of the TRAC-PF1/Mod2 model is illustrated in Figure 5.1. The active fuel zone is modeled by ROD 231 which transfers heat to the air in PIPE Component 130. The fuel rod heat structure includes UO_2 pellet, the helium gas gap, and the zircaloy cladding. The hot air that rises from the bundle is replaced by air that circulates down the sides of the SFP to the bottom of the spent fuel storage cell. The relatively cool air drops down in the opening in the SFP (represented by PIPE Component 110), runs under the SFP rack (represented by PIPE Component 120), and rises through the fuel bundle. The geometric and boundary conditions in the BREAK components were specified as identical (i.e., same elevation, flow area, and flow length). The pressure was set to 14.7 psia. Dry air properties were conservatively specified to minimize the heat capacitance of the gas. The flow was entirely driven by a natural circulation flow pattern (i.e., no forced flow conditions). A further discussion of the flow inlet boundary conditions is presented in Section 5.2.3.

The resistance through the fuel bundle is the same as used in the MELCOR simulation. The key resistance parameters are summarized in Table 5.1. At the bottom of the model (i.e., PIPE 120, Cell Face 3, see Figure 5.1), the equivalent resistance for the flow losses under the rack, including the Bernoulli effect, was added (see Section 5.2.3). The cell divisions in the bundle (i.e., PIPE 130) were explicitly placed to accurately represent the tie-plate and grid-spacer locations.

[9] The limiting location refers to the location that led to the highest exit temperature in the FLOW-3D® calculation. The limiting location (i.e., near the leading edge of the opening of the northeast region of the SFP) had the lowest flowrate due to an entrance Bernoulli flow effect.

Table 5.1 TRAC-PF1/Mod2 Bundle Resistance Parameters.

Parameter	Value	Reference
Inlet + Lower Tie-plate K Term[a]	7.56	[11]
7 Grid Spacers K Terms[a]	7 x 1.38	
Upper Tie-plate K Term[a]	1.41	
Number of Rods/Bundle	64	[10]
Number of Bundles	2884	[6]
Flow Area/Bundle [ft^2]	0.111	[10]
Rod Length [ft]	12.1 (Heated)	
Hydraulic Diameter ($4\ A/P_W$) [ft]	0.0452	
Wall Roughness [ft] – Drawn tubing	5e-6	[12]

Note (a). K resistance based on channel flow area.

The axial power distribution was evaluated from plant measurements of the axial burn-up [6]. The power profile was non-dimensionalized and input into the TRAC-PF1/Mod2 ROD model. Figure 5.2 shows the peak axial power factor of 1.19 at the Node 11 (from the bottom). However, the power profile is relatively flat between Nodes 4 and 18. The complete 24 node power profile was entered into the TRAC-PF1/Mod2 ROD model. The bundle power was internally distributed across the 8 eight heated nodes of the fuel rods. The unheated portion of the rod above the active fuel was not modeled nor was the water rod. Since rod-to-rod power variations are not expected in a high burn-up bundle, all 63 fueled rods were modeled with the same power. However, a sensitivity calculation was performed (see Section 5.3) where the power in all 63 rods was increased to a hot rod peaking factor for a beginning-of-life fuel bundle.

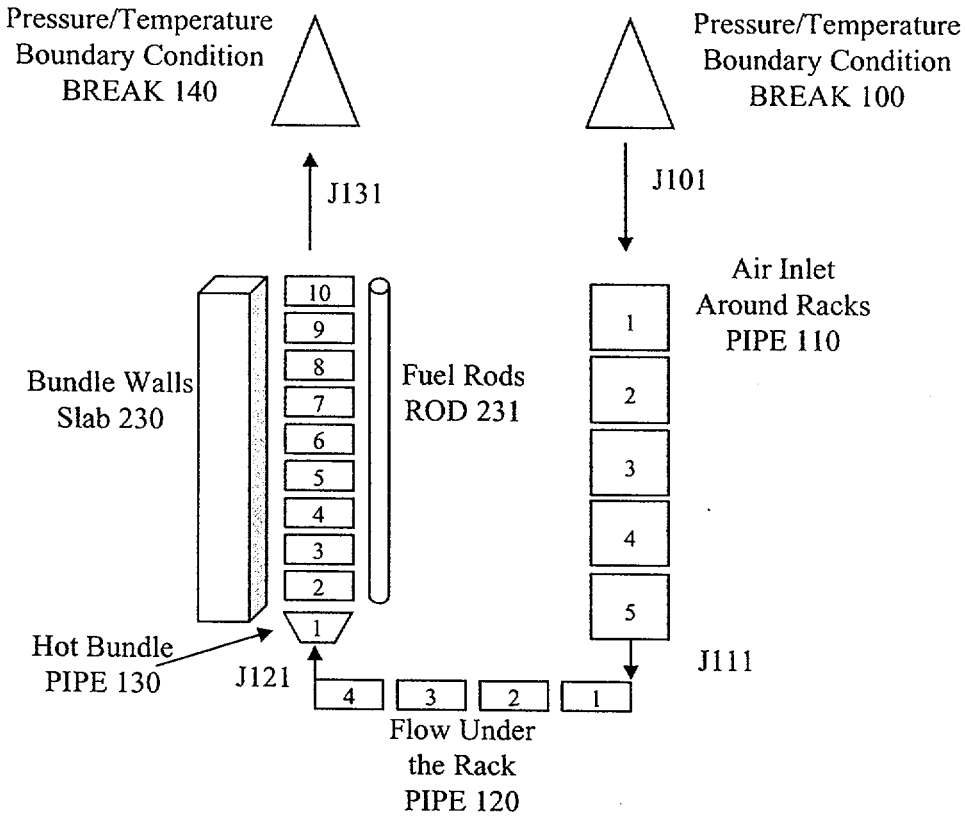

Figure 5.1 Schematic of the TRAC-PF1/Mod2 Model of a Hot Bundle in the SFP.

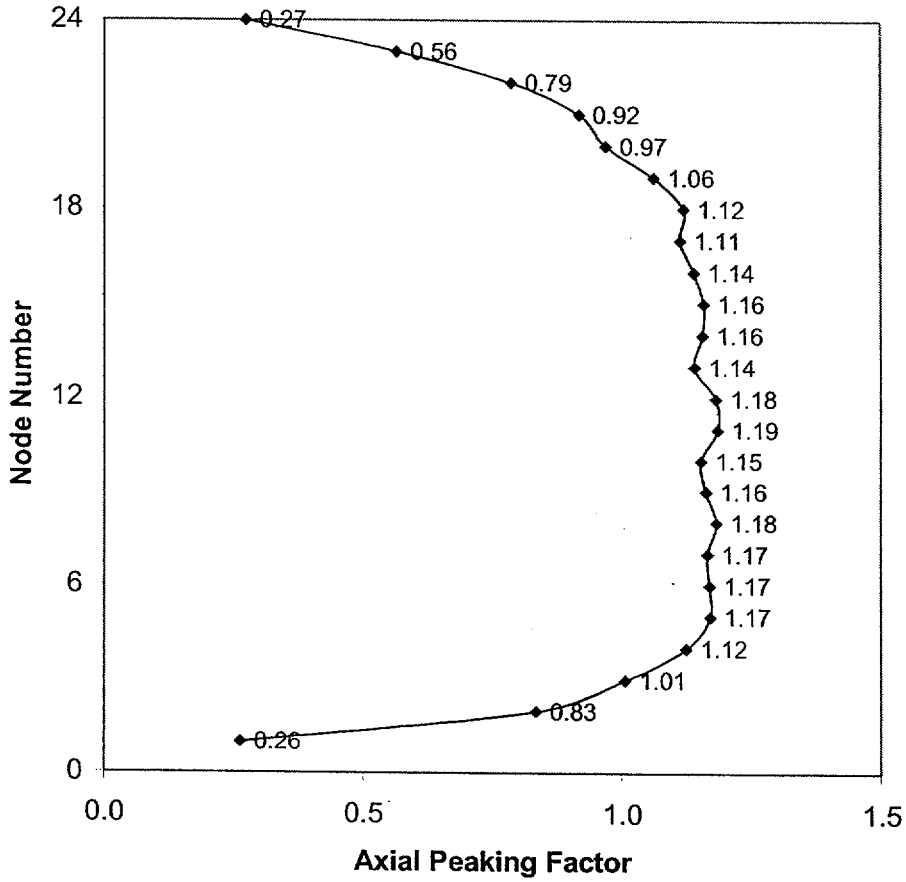

Figure 5.2 Core Axial Peaking Factor.

5.2.2 Maximum Assembly Decay Heat Selection

The Millstone 1 SFP contains spent fuel bundles from fifteen fuel cycles [6]. Within a cycle, variations in burn-up and initial uranium loading are also present. Variations in these parameters lead to different levels of heat-producing decay reactions. However, as the fuel ages in the SFP, the heat produced by the decay reactions decreases. A key parameter affecting the thermal-hydraulic results was the amount of decay heat in the bundles. Therefore, the criteria used to identify the highest decay heat level included the minimum cooling time, the maximum burn-up (i.e., integrated power experienced during residence in the reactor), and the highest uranium enrichment loading. The analysis of this "limiting case" bundle would bound the fuel cladding temperature responses for the lower powered bundles.

Spent fuel bundles discharged at the End of Cycle 15, when the power plant was last shutdown, would have the smallest number of days of decay since discharge. The fuel bundles with the highest relative powers during the previous cycle would initially have the highest heat load, but this heat load is mostly attributed to short-lived gamma decay. The fuel from Cycle 15 has been discharged since November 8, 1995 (~4 years to September 1, 1999), and this is more than enough time for short-lived effects to decay. Consequently, the most recently discharged fuel with the highest average burn-up would represent the maximum heat load in the SFP. The fuel assembly with the highest burn-up is LYS-108 with 37,240 MWD/MTU. This bundle is one of the 196 bundles in the LYS batch from Cycle 15.

An ORIGEN2 calculation for the LYS-108 bundle was not made. Rather, ORIGEN2 calculations were made based on the average characteristics of the batches loaded in the core. The decay heat for the limiting LYS-108 bundle was linearly extrapolated from decay heat calculations for the LYS batch. This procedure was appropriate because:

1) the reload fuel batches were of a similar design and varied by a small range in initial enrichment and gadolinia content,
2) the cooldown periods have been long enough to eliminate the short-lived gamma decay effects (over >1 year), and
3) the burn-up extrapolation was relatively small compared to the range of burn-up data in the database used for extrapolation.

The correctness of this procedure was verified by examining the relationships of the decay heat to burnup for the highest exposed fuel batches. The fuel design and decay heat characteristics of the three highest batches from Cycle 15 are shown in Table 5.2. The average LYS batch decay heat[10] was between the LYH and LYX batch average decay heats. The last two columns of Table 5.2 show the ratios of the LYS and LYX burn-up and decay heats to the LYH batch. To two significant digits, the decay heat scaled identically with the fuel burn-up. The scaling results are shown graphically in Figure 5.3.

[10] Assembly LYS-108 was in the LYS batch.

Next, the decay heat for LYS-108 was estimated. Using the LYH batch average values as the basis for linear scaling, the LYS-108 decay heat on January 1, 1999 was estimated as,

$Q_{Decay\ Heat,\ LYS\text{-}108}$ = (Burn-up of LYS-108 / Burn-up of LYH Batch) * $Q_{Decay\ Heat,\ LYH\ Batch}$

$Q_{Decay\ Heat,\ LYS\text{-}108}$ = (37,240 MWD/MTU / 34,340 MWD/MTU) * 1,550 Btu/hr

$Q_{Decay\ Heat,\ LYS\text{-}108}$ = (1.08) * 1,550 Btu/hr = 1,681 Btu/hr

Alternately, using the LYS batch average values as the basis for linear scaling, the LYS-108 decay heat on January 1, 1999 was estimated as,

$Q_{Decay\ Heat,\ LYS\text{-}108}$ = (Burn-up of LYS-108 / Burn-up of LYS Batch) * $Q_{Decay\ Heat,\ LYS\ Batch}$

$Q_{Decay\ Heat,\ LYS\text{-}108}$ = (37,240 MWD/MTU / 33,580 MWD/MTU) * 1,511 Btu/hr

$Q_{Decay\ Heat,\ LYS\text{-}108}$ = (1.11) * 1,511 Btu/hr = 1,675 Btu/hr

The estimated decay heats for the LYS-108 bundle (i.e., 1,681 Btu/hr or 1,675 Btu/hr) were in good agreement whether LYS or LYH batch average results were used as the basis for scaling.

Proceeding with the scaling results that used the LYS batch average properties, the LYS-108 bundle decay heat for September 1, 1999 was calculated in Table 5.3. This was done by applying a 1.08 scaling factor (i.e., the ratio of the LYS-108 bundle burn-up to the LYH batch average burn-up from the calculation above) to the LYS batch average decay heats. As of September 1, 1999 the LYS-108 bundles had 1,397 days of decay and an estimated decay heat of 1,384 Btu/hr. Both the LYH and LYS batches have the General Electric designation, G8B-P8DQB338-11GZ-80M-145-T. They are an 8x8 design with an active heated length of 145" [6].

Table 5.2 Comparison of Cycle 15 Batch Average Decay Heat and Burn-ups.[a]

Batch Designation	Number of Bundles	Enrichment [%]	kg of U per Bundle	Batch Ave Burn-up [MWD/MTU]	Decay Heat [Btu/hr]	Ratio of LYH Burn-up	Ratio of LYH Decay Heat
LYH	8	3.36	177.4	34,340	1550	1.00	1.00
LYS	196	3.38	177.4	33,580	1511	0.98	0.98
LYX	188	3.14	172.3	26,920	1206	0.78	0.78

Note: (a). From Reference [5]. Only high burn-up batches shown (i.e., above 20,000 MWD/MTU).

Table 5.3 Calculation of Peak Assembly Decay Heat.

Date	Number of Days Since Discharge to SFP	LYH Batch Average Decay Heat [Btu/hr]	Ratio of LYH Batch Average and LYS-108 Burn-up	LYS-108[b] [Btu/hr]
1-Jan-99	1154	1550	1.08	1,681
1-Sep-99	1397	1276[a]		1,384[a]
1-Jan-00	1519	1185		1,286

Notes: (a). Conservatively based on a linear interpolation between 1/1999 and 1/2000.
(b). LYS-108 decay heat is calculated based on multiplying the LHS batch average decay heat times the ratio of the LYH and LYS-108 burn-ups.

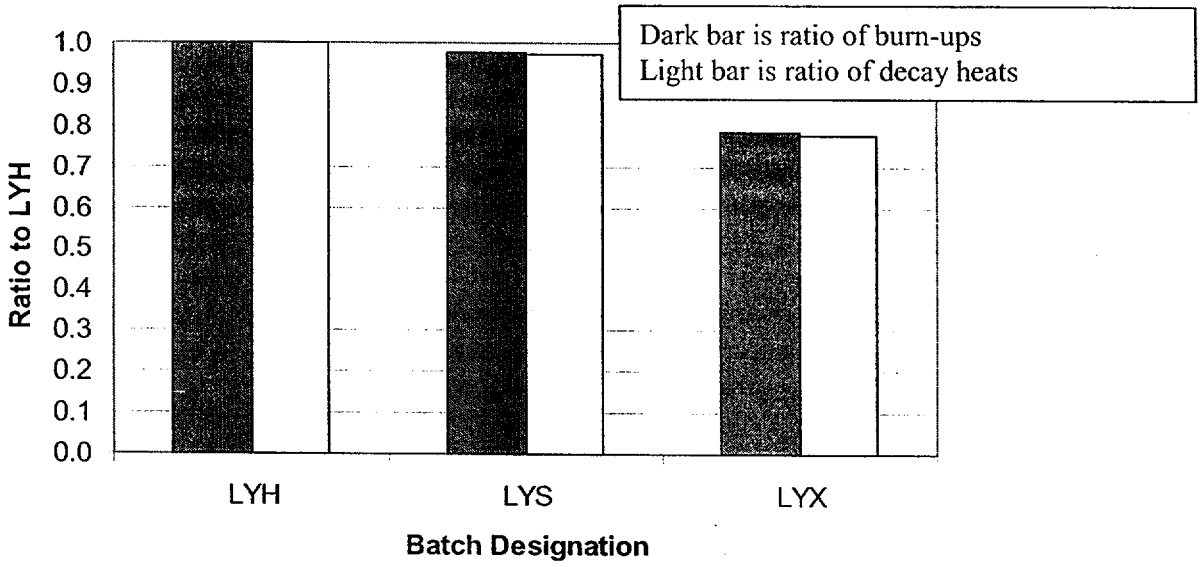

Figure 5.3 **Comparison of the Ratio of Cycle 15 Batch Average Bundle Burn-ups to the Ratio of Decay Heats.**

5.2.3 Inlet Boundary Conditions

In addition to the bundle decay heat, the other two key boundary conditions for the TRAC-PF1/Mod2 model are the inlet gas temperature and the inlet flow rate. The inlet gas temperature was obtained by combining the MELCOR and FLOW-3D® results. As shown below, the TRAC-PF1/Mod2 bundle inlet temperature was determined from both the peak bulk temperature from the MELCOR calculation (i.e., the peak building temperature was conservatively rounded up to 71°C (160°F), see Section 3.3) and the temperature rise between the bulk building temperature and the limiting bundle inlet from the FLOW-3D® calculation (i.e., 11°C, (20°F) see Section 4.3).

$$T_{Inlet} = T_{Bulk\ from\ MELCOR} + \Delta T_{FLOW\text{-}3D}$$

$$T_{Inlet} = 71°C + 11°C = 82°C$$

The resultant temperature is the inlet condition and it accounts for bulk heating effects as well as mixing at the exit of the SFP racks.

The flow resistance at the bottom of the manometer (i.e., PIPE 120) was balanced to match the limiting location inlet flow conditions from the FLOW-3D® simulation (i.e., 0.49 ft/s, which results in a flowrate of 12.4 lbm/hr) at the limiting bundle location. Figure 5.4 shows a comparison of the TRAC-PF1/Mod2 limiting bundle location benchmark calculation to the FLOW-3D® result. The TRAC-PF1/Mod2 benchmark calculation used the same power density and bundle inlet temperature as calculated in the FLOW-3D® calculation for the hottest bundle location. The resistance under the racks in the TRAC-PF1/Mod2 model was adjusted to give a bundle inlet flow equal to the FLOW-3D® result. As shown in Figure 5.4, the resulting calculated exit gas temperature from TRAC-PF1/Mod2 is in excellent agreement with the FLOW-3D® result. The flow resistance under the racks was held constant for the peak cladding temperature calculations presented in Section 5.3.

As described above, the TRAC-PF1/Mod2 flow resistance was balanced to give the same flow characteristics as the limiting bundle location in the FLOW-3D® calculation. The power density for the FLOW-3D® calculation conserved the highest batch average bundle power across the physical area represented by the six high-powered bundles. However, the physical area represented by the six high-powered bundles included spacing for air gaps in the rack structure. Therefore, the FLOW-3D® power represented a lower power density than would be represented in a single bundle model. Consequently, the TRAC-PF1/Mod2 calculations described in Section 5.3 were performed to better represent the maximum decay heat level as well as to determine the fuel cladding temperature response. The TRAC-PF1/Mod2 model applied the decay heat explicitly to the UO_2 in the sixty-three powered rods (the water rod was unpowered). The decay heat from the hottest bundle (i.e., the LYS-108, see Section 5.2.2) and a scenario date of September 1, 1999 was used (i.e., 1,384 Btu/hr, see Table 5.3).

5.2.4 Modeling Assumptions and Conservatisms

Several assumptions were made during the development of the TRAC-PF1/Mod2 model for this analysis. These assumptions are listed below.

1. The TRAC-PF1/Mod2 model was initiated at the peak inlet temperature described in Section 5.2.3. Since the full transient took nearly 50 days to reach the peak bulk temperature condition (see Section 3.3), the timing on the TRAC-PF1/Mod2 is very conservative. The purpose of the TRAC-PF1/Mod2 calculation was to determine the peak cladding temperature, not the transient time.

2. The effects from zircaloy oxidation and clad ballooning were not considered. Although this is a non-conservative assumption, the resulting peak cladding temperature was below 565°C. Therefore, neither clad ballooning nor the onset of rapid oxidation would occur and therefore was not important to model.

3. The effects of all heat transfer modes (i.e., radiation, conduction, and convection) to adjacent bundles or the rack structures were ignored. This conservatively maximized the bundle peak cladding temperature.

4. The flow resistance in PIPE 120 under the SFP racks was balanced to match the inlet flow conditions for the limiting case location from the FLOW-3D® calculation. This ensured the limiting bundle inlet conditions with the highest Bernoulli effect were present for the TRAC-PF1/Mod2 calculation. Once the resistance was balanced to the FLOW-3D® results, it was held constant for all the calculations.

5. All the decay heat was put into the 63 heated rods. The water rod was conservatively omitted as was the unheated portion of the fuel rods at the top of the fuel bundle. However, the hydraulic resistance for the water rod and the unheated portion of the fuel rods was included in the model.

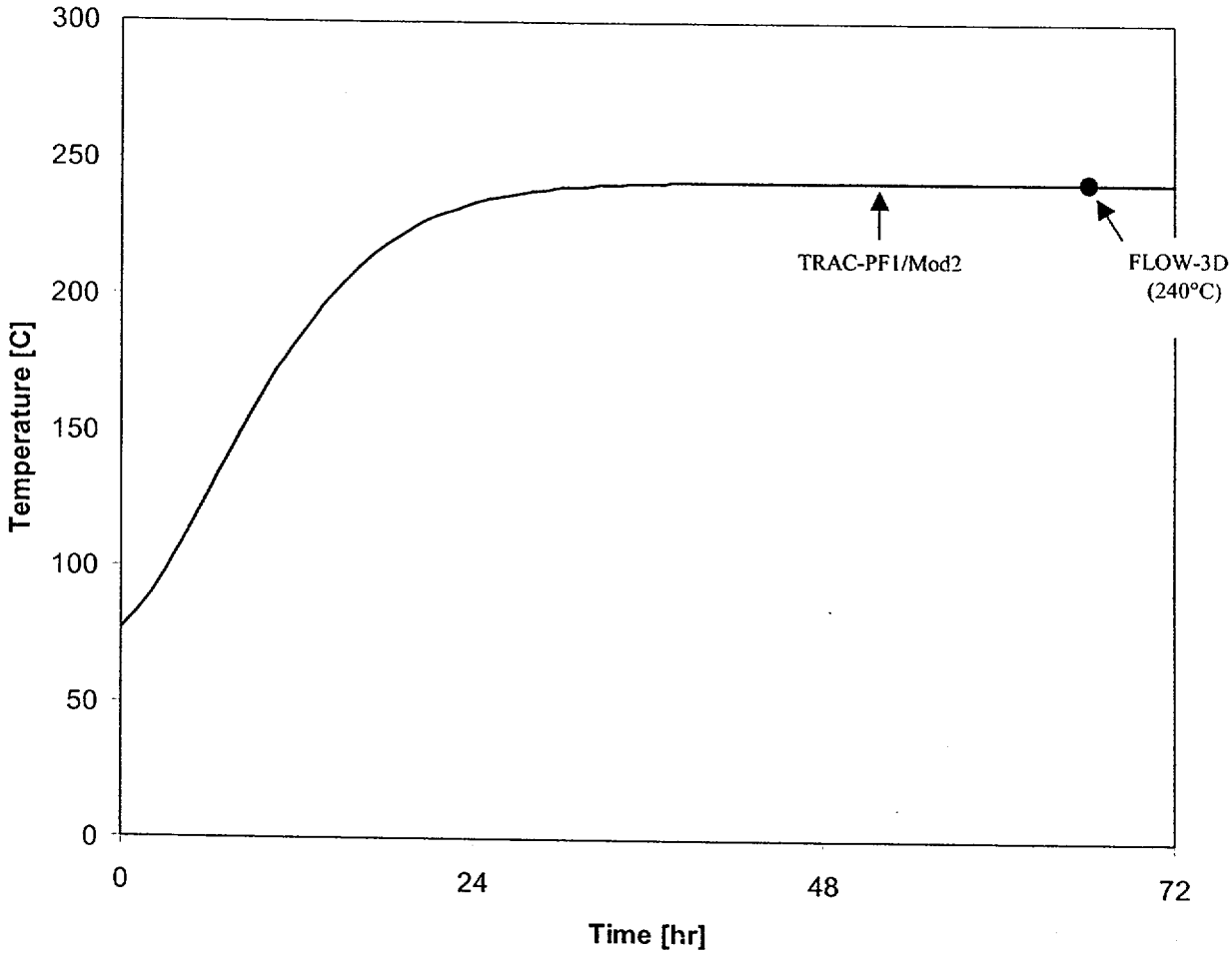

Figure 5.4 **Comparison between TRAC-PF1/Mod2 and FLOW-3D® Exit Gas Temperatures at the Limiting Bundle Location.**

5.3 TRAC-PF1/Mod2 Calculations

Three TRAC-PF1/Mod2 calculations were performed using the single bundle model. As shown in Table 5.4, the three calculations varied the bundle decay heat and the flow losses in the bundle. Calculation 1 is considered the base calculation. Calculation 1 conservatively represents the response of the highest-powered bundle in the limiting location. The response of all other bundles (including LYS-108 at a different location) is bounded by this calculation. While BWR fuels typically have a small amount of rod-to-rod peaking (i.e., <1.1), the peaking factor flattens as the bundle burns up. Consequently, the decay heat from all the rods in Bundle LYS-108 would be expected to be equal (i.e., Calculation 1). Nevertheless, a second calculation was performed using a 1.1 multiplier to the decay heat. This multiplier was applied to all of the rods in the bundle to conservatively account for any possible hot rod effects. Finally, a third calculation was performed with an increase in the bundle flow losses. The inlet, tie-plate, and seven grid spacer losses were all doubled. In addition, the wall roughness was increased from a value consistent with drawn tubing (5.e-6 m) to one consistent with commercial steel (1.5e-5 m). This conservatively increased the flow resistance to account for any uncertainties in the flow losses or laminar wall drag.

Table 5.4 Summary of TRAC-PF1/Mod2 Calculations.

Calculation	Decay Heat [Btu/hr]	Bundle Losses	Inlet Temperature	Comments
1	1,384	Nominal	82°C (180°F)	Average Rod Base Model
2	1,522			Hot Rod Model
3	1,522	2 X		Hot Rod + Additional Losses

Table 5.5 and Figure 5.5 summarizes the results from the three calculations. The base case calculation gave a peak cladding temperature of 325°C (617°F). When the decay heat was conservatively increased by 1.1 to simulate all hot rods, the peak cladding temperature of increased by 19°C (34°F) to 344°C (651°F). Finally, when the hot rod decay heat and additional flow losses both were applied, the peak cladding temperature increased to 347°C (656°F). These three values are far below the acceptance criteria of 565°C.

A hand check of the HTC was made for Calculation 3. The local Reynolds Number was 105. Using the laminar forced convection HTC of Sieder and Tate [19], the HTC is 0.62 Btu/(h-ft^2-°F). This is larger than the value calculated by TRAC-PF1/Mod2 at the peak cladding temperature location (i.e., 0.38 Btu/(h-ft^2-°F)). The lower HTC in TRAC-PF1/Mod2 is conservative because it leads to higher fuel cladding temperatures. Neglecting other effects in the flow solution and applying the Sieder and Tate laminar HTC, the peak cladding temperature

would lower by ~3°C (5°F)[11]. As can be seen, this change is inconsequential and small uncertainties in the HTC are not significant.

Table 5.5 Summary of TRAC-PF1/Mod2 Results.

Calculation	Decay Heat [Btu/hr]	Bundle Losses	Inlet Temperature	Exit Temperature	Peak Cladding Temperature
1	1,384	Nominal	82°C (180°F)	319°C (606°F)	325°C (617°F)
2	1,522			337°C (639°F)	344°C (651°F)
3	1,522	2 X		340°C (644°F)	347°C (656°F)

Finally, discussions with the Millstone 1 staff revealed that several fuel bundles have clips that hung up on the racks such that they were not completely lowered to the base of the racks. As shown in Reference [20], the bundles were identified to be raised about 1 to 3 inches above the base of the racks. A sensitivity calculation was performed with TRAC-PF1/Mod2 assuming the spacing between the bundle nose-piece and the hole at the base of the rack caused additional abrupt contraction and expansion losses equal to 1.5 [12], based on the nose-piece flow area. Using the other boundary conditions from Calculation 3, it was determined that there was essentially a negligible effect of the peak cladding temperature (<1°C). This was not surprising because the flow velocity was very low and the additional flow losses due to the expansion and contraction about the rack inlet were a small effect (see Calculation 3 effect).

[11] The change in cladding temperature was estimated by taking the ratio of the Sieder and Tate laminar heat transfer coefficient and the TRAC-PF1/Mod2 value times the rod-to-gas temperature difference (i.e., 7°C). Since the rod-to-gas heat transfer coefficient is relatively low, the impact on the peak cladding temperature is not significant.

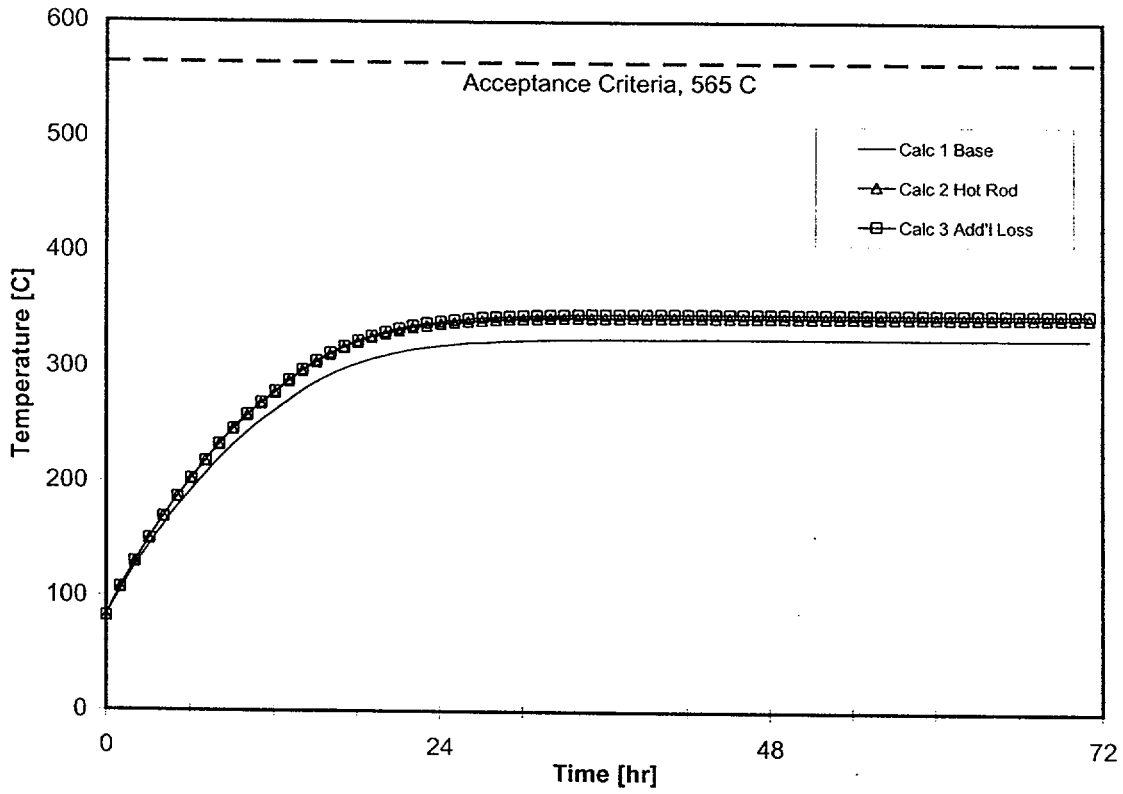

Figure 5.5 Maximum Clad Temperature for the Highest Powered Bundle in the Limiting Location for the Three TRAC-PF1/Mod2 Calculations.

6. CONCLUSIONS

An analysis of a loss-of-coolant inventory scenario was performed for the Millstone 1 SFP. The analysis used a three-level approach to accurately capture the scale of the phenomena present in the scenario. For the purposes of specifying the SFP decay heat level, the scenario was assumed to occur on September 1, 1999.

First, a MELCOR calculation was run to assess the bulk building response in the room above the SFP. The MELCOR calculations considered the effects of ventilation and ambient heat loss. Assuming an unvarying ambient temperature of (41°C) 105°F, the bulk peak room temperature was reached at 69°C (156°F) after 50 days. This was conservatively rounded up to 71°C (160°F).

Next, 3-dimensional flow calculations in the SFP were performed using FLOW-3D®. The FLOW-3D® analysis identified the "limiting bundle" location at the leading edge of the rack on the northeast corner of the SFP. This location had the lowest flow due to a "Bernoulli" effect from the relatively high-speed flow entering under the rack (see Figure 6.1 for location). This calculation also showed mixing of the hot gases exiting the SFP racks with the relatively cool air entering the SFP. Due to the mixing, the gas temperature at the inlet to the "limiting bundle" was 11°C (20°F) above the bulk air temperature.

Finally, TRAC-PF1/Mod2 single bundle calculations were performed assuming that the highest power bundle was at the limiting bundle location. The TRAC-PF1/Mod2 results show that the peak cladding temperature was only 325°C (617°F) based on decay heat values from ORIGEN2 calculations for September 1, 1999. Even if (a) a hot rod peaking factor was applied to all the fueled rods in the bundle, (b) the bundle loss coefficients were increased by a factor of 2, and (c) the wall roughness was tripled, the peak cladding temperature was only 347°C (656°F).

6.1 Comparison to Acceptance Criteria

The NRC staff has given guidance that 565°C is a conservative minimum peak cladding temperature that might lead to a sustained, rapid oxidation reaction. While 565°C is not a sufficiently high temperature to cause a rapid oxidation reaction, cladding swelling could eventually lead to flow blockages that may result in decreased cooling and progressively higher cladding temperatures. Consequently, a goal of the present calculations was to evaluate whether the peak fuel cladding temperature in the limiting bundle remained below 565°C. The present analysis for Millstone 1 SFP shows that the peak cladding temperature for the hottest rod in the highest powered bundle in the limiting location was 218°C below the 565°C threshold. Consequently, the Millstone 1 SFP is not susceptible to a rapid fuel cladding oxidation reaction in the event of a loss-of-inventory accident.

6.2 Summary of Key Conservatisms

Numerous conservatisms were applied to SFP analysis to maximize the prediction of the peak cladding temperature. These conservatisms were identified in the respective MELCOR, FLOW-3D®, and TRAC-PF1/Mod2 calculations. The key conservatisms are summarized here.

1. The scenario assumed unvarying (i.e., no diurnal variations), limiting-case summer conditions for over 50 days.

2. The RB ambient heat loss assumed quiescent conditions for over 50 days. Consequently, the heat loss was limited to natural convection. In addition, air flow and heat loss to portions of the RB below the SFP floor were neglected.

3. Since September 1, 1999, all the new fuel assemblies (~190) were recently removed from the unpowered "Boraflex Racks - II" region (see Figure 6.1). The removal of the new fuel created a large, low resistance flow path to the bottom of the SFP racks (see Figure 6.1). The flowrate from the new fuel region is expected to increase and the flowrate from the large opening in the Northeast section of the SFP is expected to decrease. The reduction of the flow near the limiting bundle is expected to lower the limiting bundle peak cladding temperature.

4. The highest-powered bundle was assumed to be in the limiting location. As shown in Figure 6.1, Bundle LYS-108 is far away from the leading edge. In fact, the first two rows of bundles along the leading edge are from Cycle 14 with an average batch decay heat of <66% of the hottest batch average from Cycle 15 [6, 18].

5. A 1.1 "hot rod" multiplier was applied to all 63 fueled rods in the highest-powered bundle. In contrast, high burn-up BWR bundles are not expected to exhibit rod-to-rod power variations.

6. The flow losses to the limiting assembly were maximized in Calculation 3. The grid spacer, tie plate, and entrance losses in the highest power bundle were doubled from the best-estimate values. In addition, the wall roughness was tripled from the best-estimate value. Higher bundle flow losses are conservative because they lower the bundle flow rate and increase the rod and air temperature.

7. The outside of the limiting bundle was assumed to be adiabatic. In addition, no radiative cooling of the rods was considered.

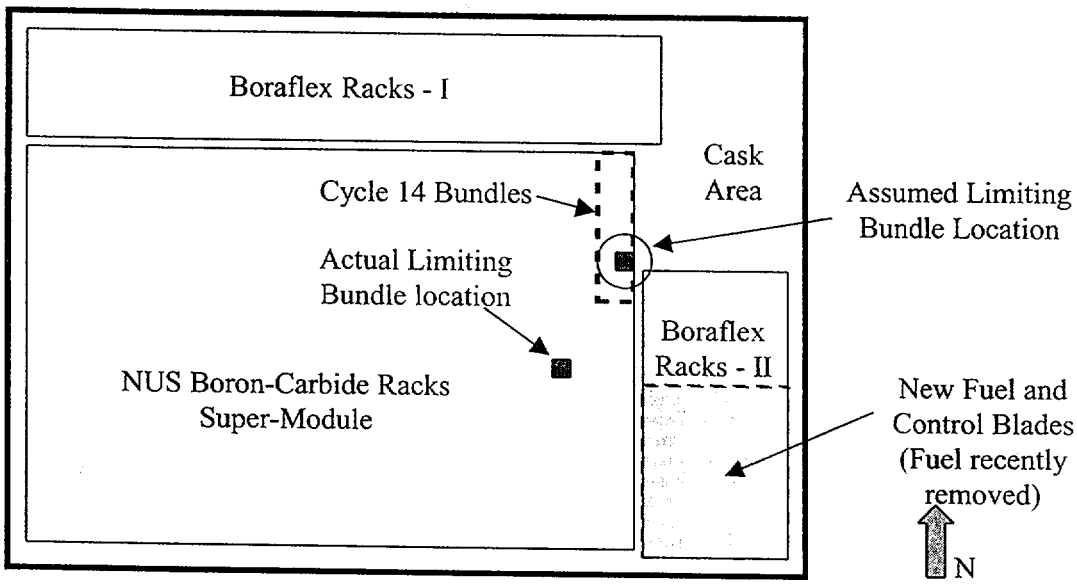

Figure 6.1 Limiting Bundle Location.

7. REFERENCES

1. US NRC, SECY-97-186, "Changes to the Financial Protection Requirements for Permanently Shutdown Nuclear Power Plants," August 13, 1997.

2. R.O. Gauntt, et al., "MELCOR Computer Code Manuals, Primer and Users' Guides, Version 1.8.4 July 1997," NUREG/CR-6119, Vol. 1, Rev. 1, SAND97-2398, Sandia National Laboratories, May 1998.

3. "FLOW-3D®, Version 7.1 User's Manual", Flow Sciences, Inc., 1997.

4. Schnurr, N. M., et al., *TRAC-PF1/Mod2 : An Advanced Best-Estimate Computer Program for Pressurized Water Reactor Thermal Hydraulic Analysis*, Los Alamos National Laboratory Report LA-12031-M, Vols. I-IV, NUREG/CR-5673, 1990.

5. "Decay Heat Load Calculation for Millstone Unit 1 Spent Fuel Pool," John Chunis and John Magyarik, 99-ENG-01905-M1, Revision 0, March 24, 1999.

6. "MP1 Spent Fuel Pool Inventory", Michael Roy, MP1SFRP-01895-F1, Revision 0, January 20, 1999.

7. US Regulatory Commission, "Regulatory Analysis for the Resolution of Generic Safety Issue 82, "Beyond Design Basis Accidents in Spent Fuel Pools," NUREG-1353, April 1989.

8. Dingman, S.E., et al., "MELCOR Analyses for Accident Progression Issues," NUREG/CR-5331, January 1991.

9. Boyack, B. E., et al., "MELCOR Peer Review," Los Alamos National Laboratory, LA-12240, March 1992.

10. Millstone Unit 1 Drawing, 25202-29119, Sheets 513-519 (NUSCO Revision 1), 521-522 (NUSCO Revision 1) and 532-534, (Revision 1).

11. Ansari, A. A., et al., "FIBER - A Steady-State Core Flow Distribution Code for Boiling Water Reactors - Code Verification & Qualification Report," EPRI-NP-1923, July, 1981.

12. Robert Fox and Alan McDonald, **Introduction to Fluid Mechanics**, 2nd Edition, John Wiley & Sons, 1978.

13. Chunis, J. and J. Magyarik, "Transient & Steady State Temperature of MP1 SFP & RB With No Active SFP Cooling," Calc. No. 99-ENG-01906-M1, Rev. 0, March 1999.

14. Millstone 1 Drawing, 25202-26035, Sheet 1, Revision 4.

15. Millstone Unit 1 Drawing, 25202-59401, Sheet 1 and 1A, Revision 2.

16. Millstone Unit 1 Drawing, 25202-29274, Sheets 3-9.

17. Millstone 1 Drawing, 25202-59401, Sheet 2, Revision 5.

18. Millstone 1 Computer Printout, Current Spent Fuel Pool, Cycle 15, Unit 1 SFP on July 21, 1998.

19. Bird, R. B., Stewart, W. E., and Lightfoot, E. N., **Transport Phenomena**, John Wiley and Sons, Inc., 1960.

20. Millstone Unit 1 Drawing, SKM-FUEL-1, April 22, 1996.

21. Duke Engineering Services, "Millstone 1 SFP Heatup Calculation", Calculation Number NU-198, November 11, 1999.